

Atom Transfer Radical Polymerization of Poly(ethylene glycol) Dimethacrylate

Qiang Yu, Faquan Zeng, and Shiping Zhu*

Department of Chemical Engineering, McMaster University, 1280 Main Street West, Hamilton, Ontario, Canada L8S 4L7

Received September 26, 2000

ABSTRACT: Reported is an experimental investigation on the atom transfer radical polymerization (ATRP) of poly(ethylene glycol) dimethacrylate (PEGDMA) initiated by an alkyl halide. The polymerization behaviors of PEGDMA in ATRP and in a conventional free radical polymerization were compared with respect to polymerization rate and gel formation. The ATRP of PEGDMA proceeded with a low rate and no observable autoacceleration, while benzoyl peroxide initiated free radical polymerization showed a strong autoacceleration from the beginning of the reaction. The radical signals, as well as copper(II) signals, in the ATRP system were observed by electron spin resonance, confirming the participation of radical intermediates in the ATRP process. At the early stage of polymerization (<40% conversion), the ATRP process proceeded in a living manner with a low and constant radical concentration. However, as the reaction continued, the increased diffusion resistance restricted the mobility of the catalyst/ligand complexes and interrupted the equilibrium between growing radicals and dormant species, resulting in a transition of the reaction mechanism to a conventional free radical polymerization process.

Introduction

Highly cross-linked polymer networks formed by the polymerization of multifunctional monomers are used for a variety of applications, such as microelectronic devices, laser video disks, coatings for optical fibers, and dental restorative materials.^{1–3} In general, multifunctional monomers exhibit some unique polymerization behavior, including prominent rate autoacceleration due to the hindered mobility of reactive chain ends.^{4–6} In addition, because of the high reaction rate and the resulting exothermic effect, along with the unequal functional group reactivity, the resulting polymeric networks are always heterogeneous.^{7–11} These structural heterogeneities severely affect the physical properties of the final cross-linked materials.

Atom transfer radical polymerization (ATRP) is a new and efficient route for synthesizing polymers with well-controlled molecular weight, low polydispersity, and novel architectures.^{12–14} The fast and reversible equilibrium between growing radicals and dormant species results in a low and constant concentration of growing radicals, which, along with the fast initiation and negligible irreversible termination, makes the polymerization proceed in a living manner. The extension of ATRP from monovinyl monomers to divinyl monomers may provide a novel approach to polymerize multifunctional monomers. With its low radical concentration and negligible termination reactions between growing radicals, autoacceleration may be reduced or eliminated and therefore produce more homogeneous polymer networks. Since the network produced by ATRP of multifunctional monomers may trap some reactive species, radical intermediates may be detected.

This work reports the ATRP of dimethacrylate oligomers, initiated by methyl α -bromophenylacetate (MBPA) with Cu(I)Br as catalyst and 1,1,4,7,10,10-hexamethyl-

Table 1. Polymerization Systems in This Work^a

system code	initiator/ catalyst system	[vinyl group] ₀ /[initiator] ₀ / [catalyst] ₀ /[ligand] ₀
BPO	BPO	100/1
ATRP-1	MBPA/CuBr/HMTETA	100/1/1/1
ATRP-2	MBPA/CuBr/HMTETA	150/1/1/1
ATRP-3	MBPA/CuBr/HMTETA	70/1/1/1
ATRP-4	MBPA/CuBr/HMTETA	50/1/1/1

^a [Vinyl group]₀ = 6.545 mol/L.

triethylenetetramine (HMTETA) as ligand. The reaction behaviors of dimethacrylate in the ATRP system and in a conventional free radical polymerization are compared with respect to polymerization rate, gel formation, and reactive species. The effects of initiator concentration and temperature on the ATRP of dimethacrylate are also discussed.

Experimental Section

Materials. Poly(ethylene glycol) dimethacrylate (PEGDMA, M_n 386 by ¹H NMR, boiling point > 200 °C/2 mmHg, glass transition temperatures (T_g) –48 °C for monomer and 32 °C for the fully cured network). Methyl α -bromophenylacetate (MBPA, 97%), copper bromide (CuBr, 99.999%), and 1,1,4,7,10,10-hexamethyltriethylenetetramine (HMTETA, 97%), all from Aldrich, were used without further purification. Benzoyl peroxide (BPO, Aldrich, 97%) was recrystallized and used as the initiator for conventional free-radical polymerization.

Sample Preparation. Take the ATRP-1 system as a real synthetic example. 2 g of PEGDMA (10.36 mmol of vinyl group), 14.82 mg of CuBr (0.1036 mmol), and 23.88 mg of HMTETA (0.1036 mmol) were added into a dried glass tube. The tube was then sealed with a rubber septum and bubbled with ultrahigh-purity nitrogen for 10 min. Initiator (MBPA, 23.73 mg, 0.1036 mmol) was then added via a degassed syringe. The solution was then shaken for 2 min prior to the DSC measurement. For the conventional radical system, 25.08 mg (0.1036 mmol) of BPO was dissolved into 2 g (10.36 mmol) of PEGDMA in a 10 mL tube reactor with stirring. The detailed polymerization systems used in this study are listed in Table 1.

Polymerization in DSC. The polymerizations were conducted in a differential scanning calorimeter (DSC, 2910, TA

* To whom all correspondence should be addressed. Phone (905) 525-9140 ext. 24962; Fax (905) 521-1350; E-mail zhuship@mcmaster.ca.

Instrument) in an isothermal mode. Approximately 25 mg of the sample mixture was put into an open aluminum pan. The DSC cell was purged with ultrahigh-purity nitrogen for 5 min prior to a temperature elevation. During the isothermal DSC scanning (70 °C for ATRP-1 and BPO systems), a 50 mL/min of nitrogen flow rate was maintained to prevent the intervention from oxygen. The rate of polymerization (R_p) was monitored by following the heat flow (dH/dt) evolved in the highly exothermic reaction and was given by eq 1.

$$R_p = (dH/dt)/\Delta H_0^{\text{theor}} \quad (1)$$

Since the reaction heat liberated in the polymerization is directly proportional to the number of reacted vinyl groups, integrating the area under the exothermic peak yields the vinyl group conversion (C),

$$C = \Delta H_t / \Delta H_0^{\text{theor}} \quad (2)$$

where ΔH_t is the reaction heat evolved up to time t and $\Delta H_0^{\text{theor}}$ is the theoretical heat of complete conversion. For methacrylates, $\Delta H_0^{\text{theor}}$ is -13.1 kcal/mol.¹⁵

GPC Measurement. The parallel polymerizations of ATRP-1 and BPO were also carried out in a water bath to extract sol polymers for molecular weight measurements by a GPC. The sample preparation followed the same procedure as for the DSC measurements. The tube was then immersed into a water bath set to 70 °C. At different time intervals, samples were taken and immediately put into THF solvent to extract unreacted monomers and sol polymers.

A Waters 590 liquid chromatography equipped with three Varian MicroPak columns (G1,000, 3,000, and 7,000HXL) and a 410 differential refractometer detector was used to measure the number- and weight-average molecular weights (M_n and M_w , respectively) of the sol fractions. THF with 2% triethylamine was used as solvent. Narrow polystyrene standards (Polysciences) were used to generate the calibration curve.

ESR Measurement. An on-line electron spin resonance (ESR) measurement was carried out in a Bruker EPR spectrometer (EP072). The spectrometer was operated at 1.59 mW power and 100 kHz of modulation frequency. An approximately 0.5 mL sample solution was transported to a 5 mm o.d. degassed ESR tube capped with a septum. The polymerization took place when the tube was inserted into the ESR cavity, which was maintained at a desired temperature with a Bruker variable temperature unit. The ESR spectra were recorded at different time intervals during the polymerization.

Radical concentrations were calculated by the double integration of the ESR spectra. A toluene solution of 4-hydroxy-2,2,6,6-tetramethylpiperidine-1-oxyl (Tempo, Aldrich) was used as a reference for the radical concentration calibration. To estimate the Cu(II) concentration, the spectra of copper(II) trifluoroacetylacetonate in toluene under the same conditions were used as reference.

Results and Discussion

1. Polymerization Behavior. Figure 1 shows the polymerization rate profiles for BPO and ATRP-1 systems, demonstrating the significant difference in polymerization behavior between these two systems. BPO-initiated polymerization of PEGDMA exhibits characteristics of a conventional free radical polymerization of multifunctional monomers.^{2,16} Because the mobility of macroradicals was severely reduced after the quick formation of a three-dimensional network at the beginning of the reaction, the bimolecular termination of the propagating radicals became difficult. The buildup of radical concentration resulted in a dramatic increase in the polymerization rate. As the reaction continued, the increased cross-linking extent also restricted the mobility of monomers, and thus the propagation reactions became diffusion-controlled. Therefore, the overall

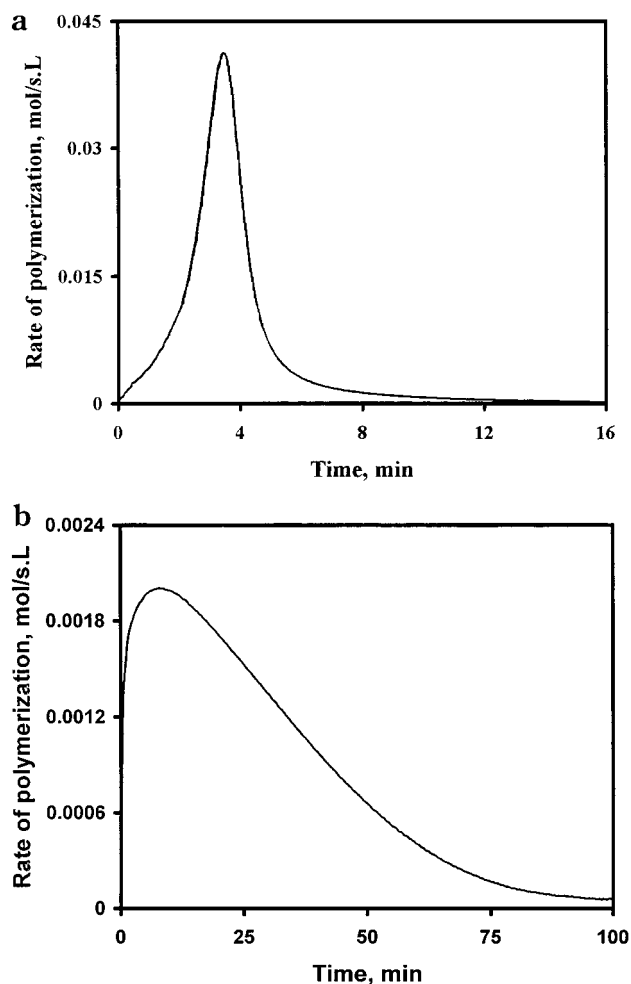
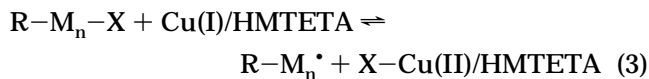


Figure 1. (a) Polymerization rate profile for the BPO-initiated polymerization of PEGDMA at 70 °C: $[\text{vinyl group}]_0 = 6.545$ mol/L, $[\text{BPO}]_0 = 0.06545$ mol/L. (b) Polymerization rate profile for ATRP of PEGDMA at 70 °C: $[\text{vinyl group}]_0 = 6.545$ mol/L, $[\text{MBPA}]_0 = [\text{CuBr}]_0 = [\text{HMTETA}]_0 = 0.06545$ mol/L.

rate of polymerization started to decrease until the reaction eventually stopped. In contrast, there was no autoacceleration in the ATRP of PEGDMA. The highest polymerization rate appeared at the beginning of the reaction. The rate decreased gradually as vinyl groups were depleted. The increased extent of reaction also decreased monomer diffusion and slowed propagation, leading to a further decrease in the rate of polymerization.

The absence of autoacceleration in the ATRP of PEGDMA in the early stage could be attributed to the low radical concentration and relatively few termination reactions between radicals. In the ATRP system, the growing radicals are in fast dynamic equilibrium with dormant species (eq 3).^{12,13}



The dormant polymeric halide, $\text{R-M}_n\text{-X}$, can be repeatedly activated by the transition metal species, Cu(I), to form the growing radical, $\text{R-M}_n\cdot$. The oxidized transition metal species, Cu(II), can further react with the radical, $\text{R-M}_n\cdot$, to regenerate $\text{R-M}_n\text{-X}$ and Cu(I). Because of the small equilibrium constant, the concentration of growing radicals is very low and the bimolecular termination of radicals is negligible. As long as

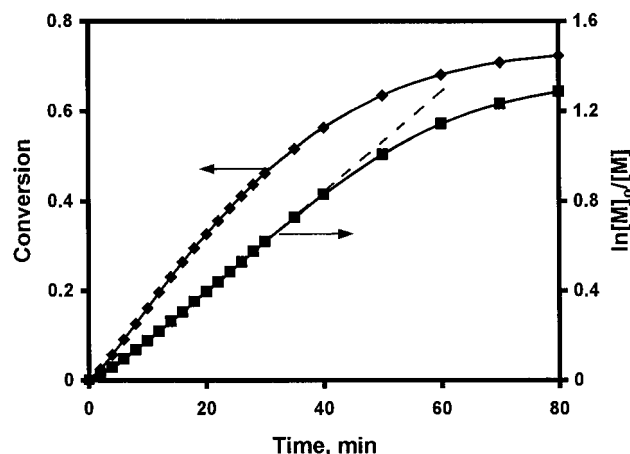


Figure 2. Kinetic curves for ATRP of PEGDMA using the same reaction conditions as in Figure 1b. The dash line indicates a linear portion of the $\ln([M]_0/[M])$ vs t curve.

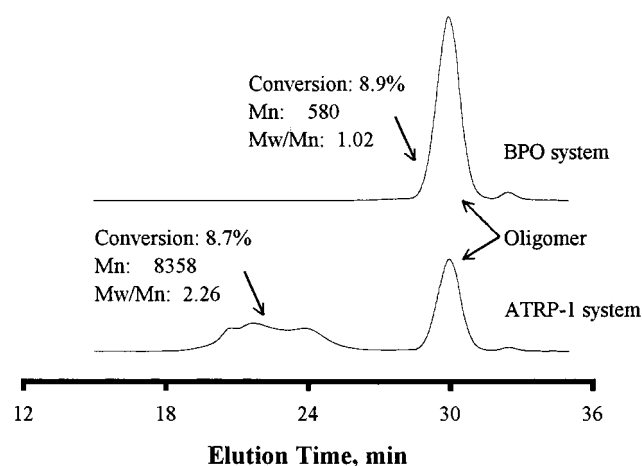


Figure 3. GPC curves for sol fractions from BPO and ATRP-1 reaction systems at 70 °C.

the transition metal species remain mobile and the reversible equilibrium is maintained, this unique mechanism would avoid the accumulation of growing radicals and eliminate autoacceleration, even in the network-forming ATRP system. Obviously, the low radical concentration also resulted in a low polymerization rate in the ATRP of PEGDMA.

Figure 2 shows the kinetic curves for the ATRP of PEGDMA with a molar ratio [vinyl group]/[MBPA]/[CuBr]/[HMTETA] = 100/1/1/1. The reaction proceeded smoothly, and the vinyl group conversion finally reached ca. 72%. Moreover, the plot of $\ln([M]_0/[M])$ vs time was linear up to 40% conversion (see the dotted line), indicating that the radical concentration remained constant in this range of the conversion. This result indicated the living character of ATRP. However, there is a remarkable deviation from linearity in the later stage of the reaction. This transition could be attributed to the restricted diffusion of catalyst/ligand complex, which will be discussed later together with the results of ESR measurements.

Gelation occurred immediately when the PEGDMA polymerization was initiated by BPO. However, there were no gels in the ATRP-1 system until the vinyl group conversion reached 5%. Figure 3 shows the GPC curves of the sol fractions of the BPO and ATRP-1 systems. The sol fraction in BPO was completely composed of unreacted PEGDMA oligomers with M_n of 580 (GPC).

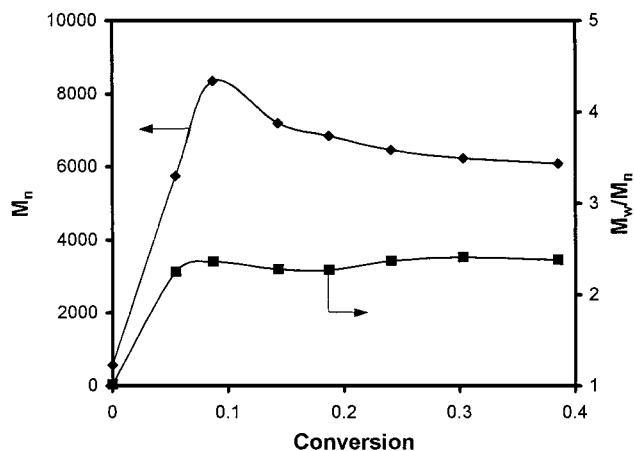


Figure 4. Variation of molecular weight and molecular weight distribution of sol polymer with vinyl group conversion for ATRP-1 at 70 °C.

However, there were two peaks in ATRP-1, indicating that the sol fraction consisted of two components, the unreacted PEGDMA oligomers and the polymer intermediates. The variation of M_n of the sol polymer in the ATRP-1 system is plotted in Figure 4. The M_n initially increased linearly with conversion, demonstrating the living nature of the ATRP process. However, after gelation, the molecular weight decreased slightly because the sol chains of high molecular weight favored network formation. The high values of polydispersity indicate that the sol polymers were highly branched.

2. Mechanism of ATRP of Dimethacrylate. The mechanism of ATRP has been extensively studied, and a radical process has been suggested.^{12,17–19} However, there is a lack of direct evidence for the involvement of radical intermediates in this process.

ESR spectroscopy is an effective tool to investigate paramagnetic species. This technique has been successfully applied to studies of free radical polymerizations, mechanical or irradiation degradation, and molecular motion.^{20,21} In a typical ATRP system, based on the proposed mechanism, a halogenated initiator reacts with Cu(I) to form a primary radical and Cu(II). The primary radical then initiates chain propagation that is controlled by the reversible deactivation of the radical with Cu(II). In this process, the radicals, as well as Cu(II), are paramagnetic and ESR-active. However, according to some ESR investigations on the ATRP of styrene,^{22,23} only Cu(II) species were observed due to its high concentration relative to the radicals. In a network-forming ATRP system, the network structure may trap reactive species. Therefore, the radical concentration in the cross-linking ATRP should be high and observable by ESR.

The BPO-initiated polymerization of PEGDMA was monitored by ESR to provide a reference. These spectra are shown in Figure 5 and have typical features of methacrylate radicals.^{24–26} The radical concentration measured by ESR vs time is shown in Figure 6. The rapid increase in the radical concentration at the beginning of the reaction corresponded to the autoacceleration region in the polymerization rate profile (Figure 1a).

Figure 7 shows the ESR spectra recorded during the ATRP of PEGDMA. The ESR signals that appeared in the first 20 min were the same as those reported in the literature^{22,23,27} and assigned to the copper(II) species. In addition to the copper(II) signal, a new signal started

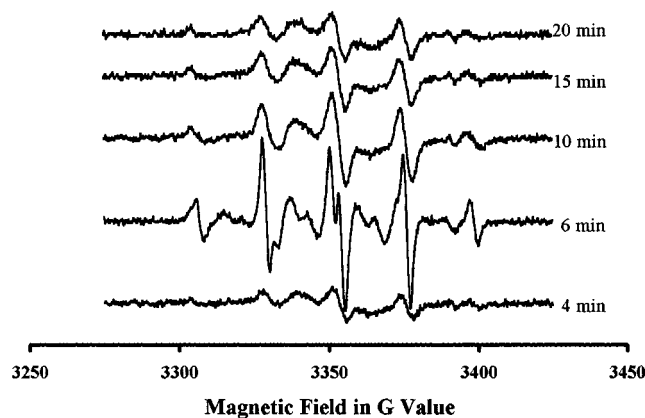


Figure 5. ESR spectra recorded during the BPO-initiated polymerization of PEGDMA at 70 °C: $[\text{vinyl group}]_0 = 6.545 \text{ mol/L}$, $[\text{BPO}]_0 = 0.06545 \text{ mol/L}$.

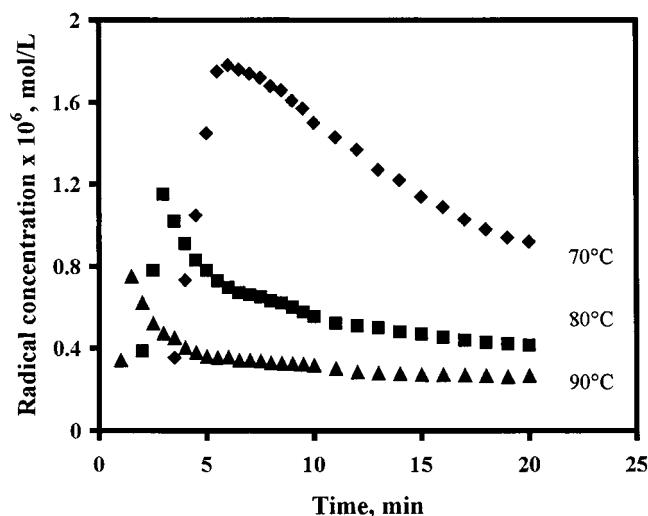


Figure 6. Variation of radical concentration measured by ESR during the BPO-initiated polymerization of PEGDMA at different temperatures: $[\text{vinyl group}]_0 = 6.545 \text{ mol/L}$, $[\text{BPO}]_0 = 0.06545 \text{ mol/L}$.

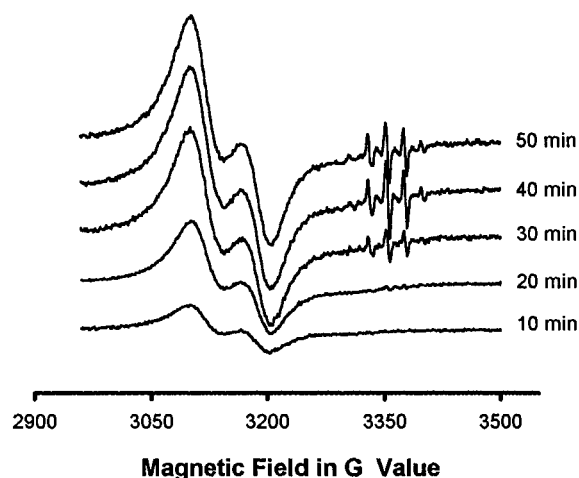


Figure 7. ESR spectra recorded during the ATRP process of PEGDMA at 70 °C: $[\text{vinyl group}]_0 = 6.545 \text{ mol/L}$, $[\text{MBPA}]_0 = [\text{CuBr}]_0 = [\text{HMTETA}]_0 = 0.06545 \text{ mol/L}$.

to appear in ca. 20 min. These signals are enlarged in Figure 8 and are typical of the nine-line methacrylate radical spectra as in Figure 5.^{24–26,28,29} This observation provides evidence that radical intermediates are involved in the ATRP process. The absence of the radical signals at the early stage of polymerization was prob-

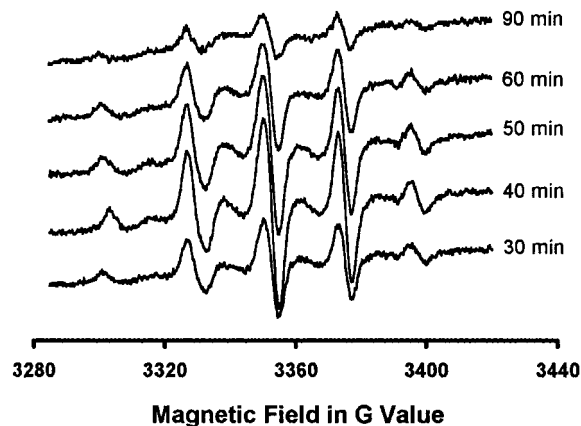


Figure 8. ESR signals from methacrylate radicals in the ATRP process of PEGDMA using the same reaction conditions as in Figure 7.

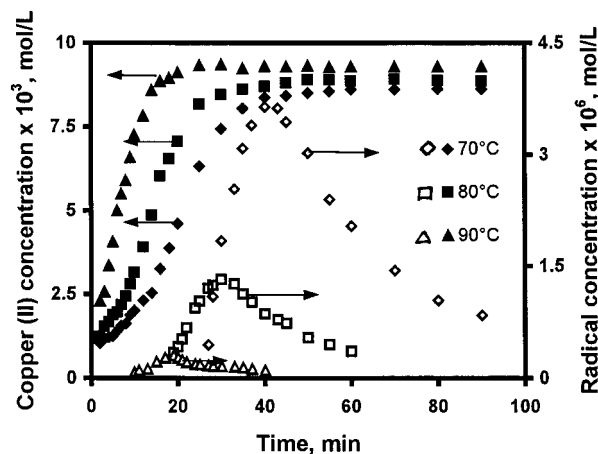


Figure 9. Copper(II) and radical concentrations as functions of reaction time for ATRP-1 system at different reaction temperatures: $[\text{vinyl group}]_0 = 6.545 \text{ mol/L}$, $[\text{MBPA}]_0 = [\text{CuBr}]_0 = [\text{HMTETA}]_0 = 0.06545 \text{ mol/L}$.

ably due to the radical concentration being below the limit of the ESR sensitivity (usually 10^{-7} mol/L).

The times required for the radical signal to appear were 28, 18, and 12 min for the ATRP of PEGDMA at 70, 80, and 90 °C. These reaction times corresponded to approximately 42–43% conversion of vinyl group (measured by DSC). Because of the network structure, diffusion of the catalyst/ligand complexes (both Cu(I) and Cu(II)) was greatly restricted. Since the deactivation reaction of R-M_n^\bullet by Cu(II) was many orders of magnitude faster than the activation of $\text{P R-M}_n\text{-Br}$ by Cu(I), the reverse reaction in eq 3 became diffusion-controlled earlier, resulting in the increase in the radical concentration. We believe this increase is due solely to the diffusion-controlled ATRP process.

The time dependence of the radical and Cu(II) concentrations in the ATRP-1 system is given in Figure 9. The Cu(II) concentration increased from the beginning of the reaction and gradually reached a steady-state concentration. Raising the temperature resulted in faster increase and higher steady-state Cu(II) concentration. The radical concentration also increased, corresponding to the increase in the Cu(II) concentration. After a maximum, it started to decrease due to significant radical termination.

The steady-state Cu(II) concentration is normally governed by the redox equilibrium. However, in the network-forming ATRP system, the steady-state Cu(II)

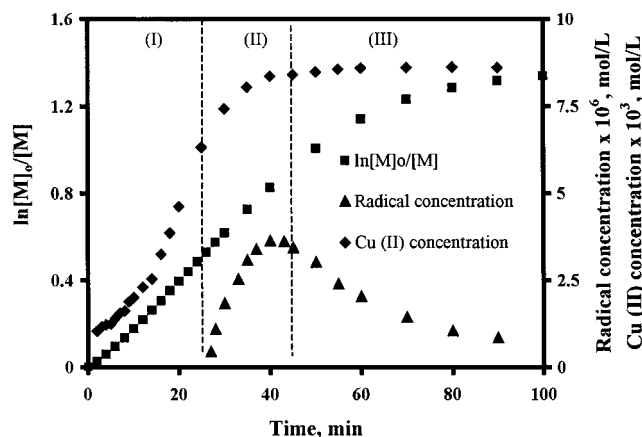


Figure 10. $\ln([M]_0/[M])$, radical concentration, and Cu(II) concentration vs polymerization time in the ATRP of PEGDMA at 70 °C: $[\text{vinyl group}]_0 = 6.545 \text{ mol/L}$, $[\text{MBPA}]_0 = [\text{CuBr}]_0 = [\text{HMTETA}]_0 = 0.06545 \text{ mol/L}$.

concentration is determined by the diffusion rate of Cu(II)/ligand complexes, which interrupts the equilibrium. The steady-state Cu(II) concentrations in this work were in the range of 0.86×10^{-2} to $0.92 \times 10^{-2} \text{ mol/L}$, i.e., approximately 13–14% conversion of Cu(I). This value is much higher than that found in the styrene ATRP system (4–6%).^{22,23}

On the basis of the above experimental observations, the ATRP of PEGDMA initiated by MBPA and catalyzed by CuBr/HMTETA complex can be divided into three stages as shown in Figure 10. At the beginning of the reaction, because of the fast equilibrium between radicals and dormant species, the radical concentration remained low and constant. The polymerization proceeded in a living manner. As the reaction continued, the mobilities of Cu(I) and Cu(II) species became gradually restricted, which impeded radical deactivation and resulted in an increase in Cu(II) and radical concentrations. Because of increasing radical concentration and the lack of protection of the radicals by copper complexes, radical termination became significant, and the living nature of the polymerization was compromised. At the final stage, the reaction behaved like a conventional free radical polymerization. The polymerization continued via the diffusion-controlled mechanism (both the copper/ligand species and monomer experienced restricted diffusion). Radical termination became dominant, resulting in the decrease of the radical concentration.

3. Effect of Initiator Concentration. A series of reactions at different MBPA concentrations were carried out at 70 °C to investigate the effect of initiator concentration on the ATRP process, with a constant initiator/catalyst/ligand molar ratio of 1/1/1. Figure 11 shows the polymerization rate profiles. Apparently, increasing initiator MBPA concentration (and catalyst CuBr concentration) increased the radical concentration. However, while the initial rate, R_{pi} , increased, the final conversion of vinyl groups decreased with increasing initiator concentration, as shown in Figure 12. We believe that the early formation of three-dimensional networks and the dense network structure at high initiator concentration were responsible for the decline of the final conversion. The densely cross-linked network trapped reactive species and stopped further polymerization.

4. Effect of Reaction Temperature. The effect of temperature on the ATRP with cross-linking was also

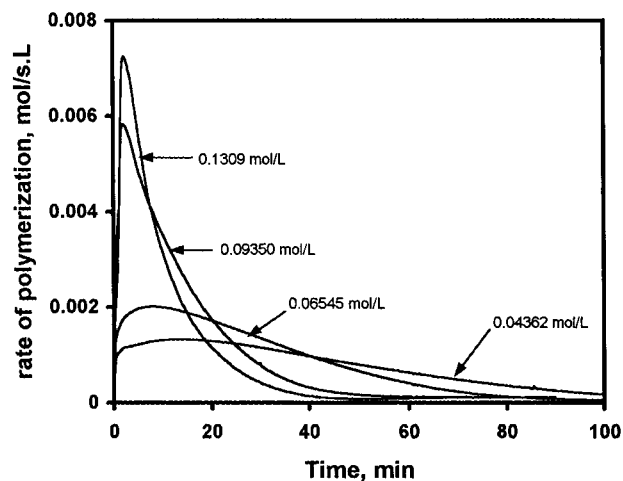


Figure 11. Polymerization rate profiles for the ATRP of PEGDMA with different initiator concentrations at 70 °C: $[\text{vinyl group}]_0 = 6.545 \text{ mol/L}$, $[\text{MBPA}]_0/[\text{CuBr}]_0/[\text{HMTETA}]_0 = 1/1/1$.

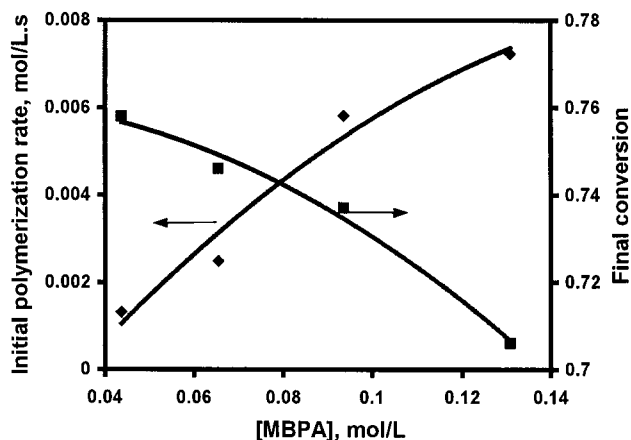


Figure 12. Influence of initiator concentration on the initial polymerization rate and the final vinyl group conversion in ATRP of PEGDMA at 70 °C: $[\text{vinyl group}]_0 = 6.545 \text{ mol/L}$, $[\text{MBPA}]_0/[\text{CuBr}]_0/[\text{HMTETA}]_0 = 1/1/1$.

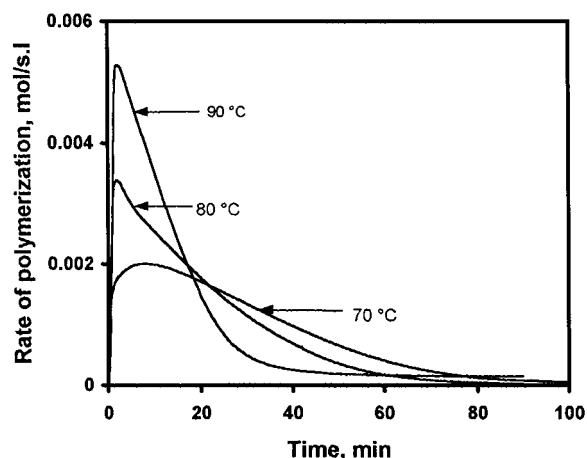


Figure 13. Polymerization rate profiles for the ATRP-1 system at different reaction temperatures: $[\text{vinyl group}]_0 = 6.545 \text{ mol/L}$, $[\text{MBPA}]_0 = [\text{CuBr}]_0 = [\text{HMTETA}]_0 = 0.06545 \text{ mol/L}$.

investigated at 70, 80, and 90 °C. The rate profiles are shown in Figure 13. Similar to the effect of the initiator concentration, the initial rate increased and the final conversion of vinyl group decreased with increasing temperature. The increase in the rate was expected

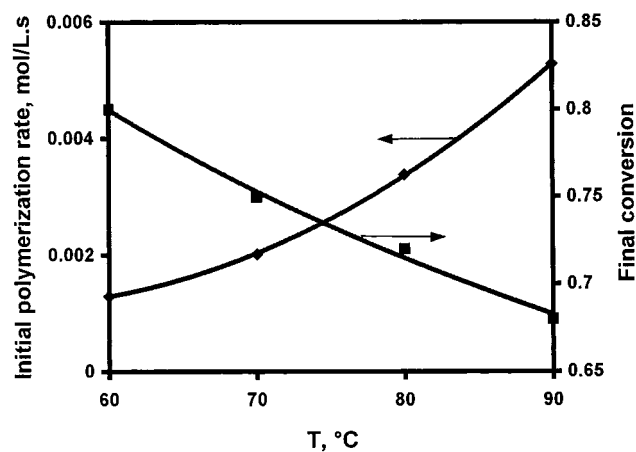


Figure 14. Effect of reaction temperature on the initial polymerization rate and the final vinyl group conversion in ATRP of PEGDMA: $[\text{vinyl group}]_0 = 6.545 \text{ mol/L}$, $[\text{MBPA}]_0 = [\text{CuBr}]_0 = [\text{HMTETA}]_0 = 0.06545 \text{ mol/L}$.

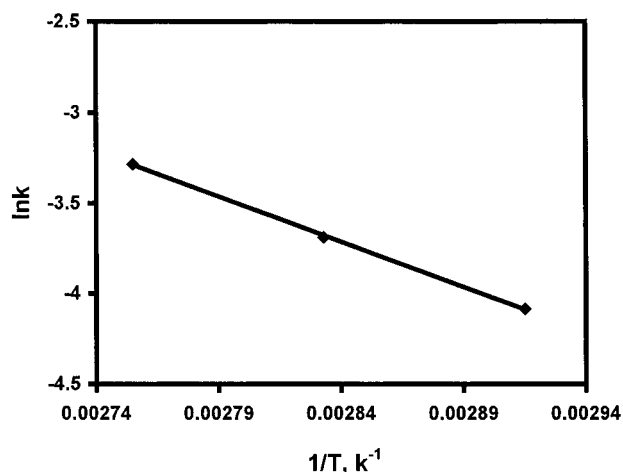


Figure 15. Arrhenius plot of the ATRP of PEGDMA using the same reaction conditions as in Figure 13.

because higher temperature enhanced the reactivity of polymeric halides, $\text{R-M}_n\text{-X}$, toward Cu(I) species, resulting in higher concentration of radicals. On the other hand, increasing temperature did not enhance the mobility of PEGDMA segments because of the low T_g value of the cured material. Nevertheless, the higher the temperature, the higher the reaction rate and the earlier the network was formed. Early network formation restricted the reactivity of vinyl groups, reducing the conversion.

The ATRP of PEGDMA at three different temperatures gave a linear relationship of $\ln[M]_0/[M]$ vs time at the first stage of the reaction. The slope of this straight kinetic plot allows one to estimate the apparent propagation rate constant, k_p^{app} .

$$R_p = -d[M]/dt = k_p[M][P^*] \approx k_p^{\text{app}}[M] \quad (4)$$

$$\ln[M]_0/[M] = k_p^{\text{app}}t \quad (5)$$

An Arrhenius curve was obtained from the k_p^{app} data (Figure 15), and the apparent activation energy, E_R , for the ATRP of PEGDMA was 41.7 kJ/mol. This value agrees with that reported (42 kJ/mol) for the ATRP of MMA.³⁰

Conclusions

The copper-catalyzed atom transfer radical polymerization of PEGDMA was investigated using DSC and

ESR. On the basis of the experimental results, the following conclusions have been drawn.

1. The ATRP of PEGDMA proceeded with very low polymerization rates, in comparison with the BPO-initiated free radical polymerization. The dynamic equilibrium between growing radicals and dormant species resulted in a lower radical concentration in the ATRP system, which avoided the accumulation of growing radicals and eliminated the autoacceleration effect.

2. Methacrylate radical signals, along with Cu(II) signals, were observed by ESR measurements. The observation of radical signals in the ATRP of PEGDMA was attributed to more restricted diffusion of the Cu(II) /ligand complex, which impeded the deactivation of growing radicals. The radical signals indicate that radical intermediates participate in ATRP.

3. At the beginning of the reaction, the ATRP of PEGDMA proceeded in a living manner because of the low and constant radical concentration. As the reaction continued, the mobility of the catalyst/ligand complex was restricted by the increased diffusion resistance, which resulted in an increase in Cu(II) and radical concentration. Thus, radical termination became significant, and the reaction was converted to a conventional free radical polymerization process. At the final stage, the polymerization continued via a diffusion-controlled mechanism.

4. The initial rate of the ATRP of PEGDMA increased, and the final vinyl group conversion decreased as the initiator concentration and/or reaction temperature increased. This apparent activation energy was 41.7 kJ/mol.

References and Notes

- Senich, G. A.; Florin, R. E. *J. Macromol. Chem. Phys.* **1984**, *C24*, 239.
- Kloosterboer, J. G. *Adv. Polym. Sci.* **1988**, *84*, 1.
- Urabe, H.; Waksas, K.; Yamaki, M. *J. Mater. Sci.: Mater. Med.* **1990**, *1*, 163.
- Kloosterboer, J. G.; Litjen, G. F. C. *Polymer* **1987**, *28*, 1147; **1990**, *31*, 95.
- Cook, W. D. *J. Polym. Sci., Part A: Polym. Chem.* **1993**, *31*, 1053.
- Allen, P.; Simon, G.; Williams, D. *Macromolecules* **1989**, *22*, 809.
- Kloosterboer, J. G.; Van deHei, G. M.; Boots, H. M. *Polym. Commun.* **1984**, *25*, 354.
- Bowman, C. N.; Peppas, N. A. *Chem. Eng. Sci.* **1992**, *47*, 1411.
- Anseth, K. S.; Newman, S. M.; Bowman, C. N. *Adv. Polym. Sci.* **1995**, *122*, 177.
- Basile, J.; Leibler, L. *Macromolecules* **1988**, *21*, 2649.
- Kloosterboer, J. G.; Litjen, G. *Macromol. Chem. Macromol. Symp.* **1989**, *24*, 223.
- (a) Wang, J. S.; Matyjaszewski, K. *J. Am. Chem. Soc.* **1995**, *117*, 5614. (b) Wang, J. S.; Matyjaszewski, K. *Macromolecules* **1995**, *28*, 7901.
- (a) Kato, M.; Kamigaito, M.; Sawamoto, M.; Higashimura, T. *Macromolecules* **1995**, *28*, 1721. (b) Ando, T.; Kato, M.; Kamigaito, M.; Sawamoto, M. *Macromolecules* **1996**, *27*, 1070.
- (a) Percec, V.; Barboiu, B. *Macromolecules* **1995**, *28*, 7970. (b) Percec, V.; Barboiu, B.; Neumann, A.; Ronda, J. C.; Zhao, M. *Macromolecules* **1996**, *29*, 3665.
- Anseth, K. S.; Wang, C. M.; Bowman, C. N. *Polymer* **1994**, *35*, 3243.
- Yu, Q.; Nauman, S.; Santerre, J. P.; Zhu, S. UV Photopolymerization Behaviour of Dimethacrylate Oligomers with Camphorquinone/Amine Initiator System. *J. Appl. Polym. Sci.*, in press.
- Controlled Radical Polymerization*; Matyjaszewski, K., Ed.; ACS Symposium Series; American Chemical Society: Washington, DC, 1998; Vol. 685.
- Greszta, D.; Mardare, D.; Matyjaszewski, K. *Macromolecules* **1994**, *27*, 638.

- (19) Matyjaszewski, K. *Macromolecules* **1998**, *31*, 4710.
- (20) Ranby, B.; Rabek, J. *ESR Spectroscopy in Polymer Research*; Springer-Verlag: New York, 1997.
- (21) Kamachi, M. *Adv. Polym. Sci.* **1987**, *82*, 207.
- (22) Matyjaszewski, K.; Kajiwar, A. *Macromolecules* **1998**, *31*, 548.
- (23) Kajiwar, A.; Matyjaszewski, K. *Macromolecules* **1998**, *31*, 5695.
- (24) Landin, D. T.; Macosko, C. W. *Macromolecules* **1988**, *21*, 846.
- (25) Tian, Y.; Zhu, S.; Hamielec, A. E.; Fulton, D. B. *Polymer* **1992**, *33*, 384.
- (26) Anseth, K. S.; Anderson, K. J.; Bowman, C. N. *Macromol. Chem. Phys.* **1996**, *197*, 833.
- (27) Hathaway, B.; Duggan, M.; Murph, A.; Mullane, J.; Power, C.; Walsh, A.; Walsh, B. *Coord. Chem. Rev.* **1981**, *36*, 267.
- (28) Zhu, S.; Tian, Y.; Hamielec, A. E.; Eaton, D. R. *Macromolecules* **1990**, *23*, 1144.
- (29) Zhu, S.; Tian, Y.; Hamielec, A. E.; Eaton, D. R. *Polymer* **1990**, *31*, 154.
- (30) Zeng, F.; Shen, Y.; Zhu, S.; Pelton, R. *Macromolecules* **2000**, *33*, 1628.

MA001665O